Published in final edited form as:
Clin Cancer Res. 2007 April 1; 13(7): 2261–2270. doi:10.1158/1078-0432.CCR-06-2468.

Synergism between Arsenic Trioxide and Heat Shock Protein 90 Inhibitors on Signal Transducer and Activator of Transcription Protein 3 Activity - Pharmacodynamic Drug-Drug Interaction Modeling

Meir Wetzler[1], **Justin C. Earp**[2], **Michael T. Brady**[1], **Michael K. Keng**[1], and **William J. Jusko**[2]
[1]Roswell Park Cancer Institute, Buffalo, NY

[2]State University of New York at Buffalo, Buffalo, NY

Abstract

Purpose—Constitutive signal transducer and activator of transcription (STAT) 3 activity, observed in approximately 50% of acute myeloid leukemia (AML) cases and associated with adverse treatment outcome, is down-regulated by arsenic trioxide (ATO). Heat shock protein (HSP) 90 is a molecular chaperone involved in signal transduction pathways. We hypothesized that HSP90 inhibitors will potentiate ATO effect on constitutive STAT3 activity and cell killing. One concern was that the effect of ATO and HSP90 inhibitors will result in up-regulation of HSP70, a protein known to inhibit apoptosis.

Experimental Design—We have used a semi-mechanistic pharmacodynamic model to characterize concentration-effect relationships of ATO and HSP90 inhibitors on constitutive STAT3 activity, HSP70 expression and cell death in a cell line model.

Results—Pharmacodynamic interaction of ATO and three HSP90 inhibitors showed synergistic interactions in inhibiting constitutive STAT3 activity and inducing cell death, in spite of a concurrent synergistic up-regulation of HSP70.

Conclusions—These preliminary results provide a basis for studying the combined role of ATO with HSP90 inhibitors in AML with constitutive STAT3 activity.

Introduction

Constitutive signal transducer and activator of transcription (STAT) 3 activity has been shown to be present in leukemia cells in 50% of acute myeloid leukemia (AML) cases and to correlate with adverse treatment outcome (1). We have shown that arsenic trioxide (ATO) down-regulates constitutive STAT3 activity in AML cells within six hours, without affecting cell survival until 48 hours (2). Heat shock protein (HSP) 90 is implicated in maintaining the conformation, stability, and function of key proteins involved in signal transduction pathways (3), and we therefore hypothesized that HSP90 inhibitors [Geldanamycin (GA), 17-allylamino-17-demethoxygeldanamycin (17-AAG) and 17-(dimethylaminoethylamino)-17-demethoxygeldanamycin (NSC 707545, 17-DMAG)] would potentiate the effect of ATO on constitutive STAT3 activity in AML cells. One concern was that up-regulation of HSP70, a

Address Correspondence to: Meir Wetzler, M.D., Leukemia Section, Department of Medicine, Roswell Park Cancer Institute, Elm and Carlton Streets, Buffalo, NY 14263, Phone: (716) 845-8447, Fax: (716) 845-2343, E-mail: E-mail: meir.wetzler@roswellpark.org.

protein known to inhibit apoptosis (4,5), by exposure to either ATO (6-8) or HSP90 inhibitors (9,10), might abrogate their effect on constitutive STAT3 activity and survival.

Identifying the type and extent of drug-drug interactions has been a challenge since the early 1900s. When the mechanisms of action of two pharmacological agents are not known, empirical drug-drug interaction models such as Loewe additivity (11), Bliss independence (12), or the Chou and Talalay method (13,14) can be applied. When the true behavior is well appreciated, mechanistic models offer insight into the physiological processes influencing the degree of interaction (15-17). The HSP90 inhibitors act by binding HSP90 and preventing the stabilization of "client" protein complexes, involving cancer targets such as mutated p53, Raf-1, ErbB2 and other proteins associated with signal transduction. On the other hand, the mechanism of ATO action towards DNA fragmentation and cell death is not completely understood. It is clear, however, that when given in combination ATO and HSP90 inhibitors may interact non-competitively through different pathways.

We examined the combined effects of each HSP90 inhibitor with ATO on constitutive STAT3, HSP70 and HSP90 protein levels using the Ariens non-competitive functional interaction model (15,16) with an interaction parameter (ψ). Interaction parameters may be useful in various mechanism-based models to account for the synergism or antagonism not predicted by the mechanistic expectations of the modeling scheme (17-19). The estimated value of this parameter indicates the intensity of the drug-drug interaction when compared to the no-interaction value (i.e. the value that does not influence the underlying mechanistic model, based on single drug effect alone). This interaction model is not limited to the level of mass-balance drug-receptor binding equations, but assumes that each drug contributes to the interaction after binding to their respective targets. Effect is assumed to be a function of bound drug-target and the Hill equation relates single drug concentrations to effect.

The cell-killing effects of ATO and 17-DMAG (currently in clinical trials) were captured in a time-dependent manner. A mechanistic drug-drug interaction model was developed, incorporating time-dependent natural cell growth and death in the system. A modified functional interaction model was used to characterize the type of interaction. These studies were designed to enhance ATO's effect on constitutive STAT3 activity.

Materials and Methods

Materials

All chemicals were purchased from Sigma Immunochemicals (St. Louis, MO) unless otherwise specified. 17-DMAG was provided by Dr. Ivy Percy, National Institute of Health, National Cancer Institute, Bethesda, MD.

Cell Line and Culture Conditions

The AML cell line, HEL, a cytokine-independent human erythroleukemia cell line that has constitutive STAT3 activity served as a model system. The cells were exposed for 6 to 48 hours to ATO, GA, 17-AAG and 17-DMAG. Cell viability was determined by the tryptan blue dye (Life Technology) exclusion assay.

Western Blotting

Tyrosine phosphorylated (P) and unphosphorylated STAT3, were quantitated by Western blot analysis as previously described (1,2,20,21). In brief, whole cell extracts were separated on 7.5% polyacrylamide SDS gels and the proteins were transferred onto nitrocellulose membranes. The membranes were incubated with antibodies (Ab) against PSTAT3 (Y705) (Upstate Biotechnology, Lake Placid, NY) and to detect nonphosphorylated proteins,

immunoblots were reacted with Ab against the N-termini of STAT3 (Transduction Laboratories, Lexington, KY) HSP70 (R & D Systems, Minneapolis, MN) and HSP90 (Santa Cruz Biotechnology, Santa Cruz, CA). The immune complexes were visualized by the enhanced chemiluminescence reaction (Amersham Life Science, Arlington Heights, IL).

Interaction Assays

All assays were conducted at least in triplicates. The Hill function was fitted to each concentration-response curve for each drug. After fitting and determination of the 50% inhibition concentration (IC_{50}), five combination ratios of the IC_{50} (ATO:HSP90 inhibitors; 1:1, 1:4, 4:1, 1.5:3, 3:1.5) were characterized.

Pharmacodynamic Drug-Drug Interaction Model

Pharmacodynamic drug-drug interactions on PSTAT3 were evaluated with the following non-competitive equation relating concentrations of both drugs to the overall effect, E.

$$\mathbf{E}=100\cdot\left[1-\frac{\mathbf{I}_{\max,\ A}\cdot\left(\frac{\mathbf{A}}{\Psi\cdot\mathbf{IC}_{50,A}}\right)^{\gamma_A}+\mathbf{I}_{\max,\ B}\cdot\left(\frac{\mathbf{B}}{\Psi\cdot\mathbf{IC}_{50,B}}\right)^{\gamma_B}+\left(\mathbf{I}_{\max,\ A}+\mathbf{I}_{\max,\ B}-\mathbf{I}_{\max,\ A}\cdot\mathbf{I}_{\max,\ B}\right)\cdot\left(\frac{\mathbf{A}}{\Psi\cdot\mathbf{IC}_{50,A}}\right)^{\gamma_A}\cdot\left(\frac{\mathbf{B}}{\Psi\cdot\mathbf{IC}_{50,B}}\right)^{\gamma_B}}{1+\left(\frac{\mathbf{A}}{\Psi\cdot\mathbf{IC}_{50,A}}\right)^{\gamma_A}+\left(\frac{\mathbf{B}}{\Psi\cdot\mathbf{IC}_{50,B}}\right)^{\gamma_B}+\left(\frac{\mathbf{A}}{\Psi\cdot\mathbf{IC}_{50,A}}\right)^{\gamma_A}\cdot\left(\frac{\mathbf{B}}{\Psi\cdot\mathbf{IC}_{50,B}}\right)^{\gamma_B}}\right] \quad (1)$$

where A refers to the concentration of ATO and B refers to the concentration of the HSP90 inhibitor (i.e. GA, 17-AAG, 17-DMAG). I_{max} is a fraction representing the maximal capacity that drug A or B may suppress total cell proliferation when administered alone. When I_{max} = 0 there is no possible inhibition and when I_{max} = 1 there may be complete inhibition of cell proliferation with sufficiently high concentrations. IC_{50} refers to the concentration of drug A alone or drug B alone that elicits the half-maximal response.

The interactions of these drugs on the stimulation of HSP70 expression was characterized by a stimulatory version of equation (1). All negative terms are made positive in this form and I_{max} and IC50 parameters take on a stimulatory meaning (i.e. S_{max}, SC_{50}).

$$\mathbf{E}=100\cdot\left[1+\frac{\mathbf{S}_{\max,\ A}\cdot\left(\frac{\mathbf{A}}{\Psi\cdot\mathbf{SC}_{50,A}}\right)^{\gamma_A}+\mathbf{S}_{\max,\ B}\cdot\left(\frac{\mathbf{B}}{\Psi\cdot\mathbf{SC}_{50,B}}\right)^{\gamma_B}+\left(\mathbf{S}_{\max,\ A}+\mathbf{S}_{\max,\ B}+\mathbf{S}_{\max,\ A}\cdot\mathbf{S}_{\max,\ B}\right)\cdot\left(\frac{\mathbf{A}}{\Psi\cdot\mathbf{SC}_{50,A}}\right)^{\gamma_A}\cdot\left(\frac{\mathbf{B}}{\Psi\cdot\mathbf{SC}_{50,B}}\right)^{\gamma_B}}{1+\left(\frac{\mathbf{A}}{\Psi\cdot\mathbf{SC}_{50,A}}\right)^{\gamma_A}+\left(\frac{\mathbf{B}}{\Psi\cdot\mathbf{SC}_{50,B}}\right)^{\gamma_B}+\left(\frac{\mathbf{A}}{\Psi\cdot\mathbf{SC}_{50,A}}\right)^{\gamma_A}\cdot\left(\frac{\mathbf{B}}{\Psi\cdot\mathbf{SC}_{50,B}}\right)^{\gamma_B}}\right] \quad (2)$$

Equation (1) was originally proposed by Ariens (15) for drugs that interact non-competitively and was modified by Chakraborty and Jusko (18) to include an interaction parameter, ψ, describing a mutual influence of each drug on the other's IC_{50} value. When ψ < 1 less total

drug is required to elicit the same response as compared to either drug administered alone. This is denoted as apparent synergy. When $\psi > 1$ more total drug is required to achieve the same maximal response and this is defined as apparent antagonism. When $\psi = 1$, there is no mutual effect on the IC_{50} value of either drug. This condition is termed no-interaction and is our reference model based on the non-competitive assumptions of Ariens' functional interaction. The stimulatory function obeys these properties as well.

In the above equations when the concentration of A or B is zero the equation reduces to the form of the basic Hill function. For example in equation (1) when concentrations of drug B equal zero

$$\mathbf{E}=100\cdot\left[1-\frac{\mathbf{I}_{\max,\ \ \mathbf{A}}\cdot\left(\frac{\mathbf{A}}{\Psi\cdot\mathbf{IC}_{50,\mathbf{A}}}\right)^{\gamma_{\mathbf{A}}}}{1+\left(\frac{\mathbf{A}}{\Psi\cdot\mathbf{IC}_{50,\mathbf{A}}}\right)^{\gamma_{\mathbf{A}}}}\right] \tag{3}$$

where ψ is assumed to be one in the absence of either drug. In equation (2) when concentrations of drug B equal zero

$$\mathbf{E}=100\cdot\left[1-\frac{\mathbf{S}_{\max,\ \ \mathbf{A}}\cdot\left(\frac{\mathbf{A}}{\Psi\cdot\mathbf{SC}_{50,\mathbf{A}}}\right)^{\gamma_{\mathbf{A}}}}{1+\left(\frac{\mathbf{A}}{\Psi\cdot\mathbf{SC}_{50,\mathbf{A}}}\right)^{\gamma_{\mathbf{A}}}}\right] \tag{4}$$

where ψ is assumed to be one in the absence of either drug.

Pharmacodynamic Drug-Drug Interaction Model for Time-Dependent Cell-Killing Data

Natural growth parameters of the system were determined by fitting the logistic function to live cell data without the presence of drug, over a 72 hour time-course. A natural cell loss term was necessary to account for the loss of cells noted in the viable cell counts reported. The underlying model for natural cell-growth in the system is:

$$\begin{aligned}&\frac{d\mathbf{X}}{dt}=k_{\mathbf{syn}}\cdot X\cdot\left(1-\frac{\mathbf{X}}{\mathbf{X}_{\max}}\right)-k_{\mathbf{nat}}\cdot\mathbf{X};\quad X(0)=500,000\quad\mathbf{cells}\\&\frac{d\mathbf{N}_D}{dt}=k_{nat}\cdot\mathbf{X};\qquad\qquad\qquad\qquad N_D(0)=0\quad\mathbf{cells}\end{aligned} \tag{5}$$

where X is the total number of live cells present, N_D is the total number of dead cells, k_{syn} is the rate constant for natural cell synthesis, X_{max} is the capacity for living cells in the culture, and k_{nat} is the first-order rate constant for natural cell death.

Cell survival data for single drug effect was best described by a linear time-dependent cell-killing model. Drug effect was modeled as a stimulation of natural cell loss.

$$\begin{aligned}&\frac{d\mathbf{X}}{dt}=k_{\mathbf{syn}}\cdot X\cdot\left(1-\frac{\mathbf{X}}{\mathbf{X}_{\max}}\right)-k_{\mathbf{nat}}\cdot\left(1+\mathbf{S}_{\max\ \ \mathbf{ATO}}\cdot C_{\mathbf{ATO}}\right)\cdot\mathbf{X};\quad X(0)=500,000\quad\mathbf{cells}\\&\frac{d\mathbf{N}_D}{dt}=k_{\mathbf{nat}}\cdot\left(1+\mathbf{S}_{\max\ \ \mathbf{ATO}}\cdot C_{\mathbf{ATO}}\right)\cdot\mathbf{X};\qquad\qquad\qquad\qquad N_D(0)=0\quad\mathbf{cells}\end{aligned} \tag{6}$$

S_{maxATO} is the stimulatory effect constant per concentration of ATO, C_{ATO}. Drug effect data for 17-DMAG was modeled in the same manner.

The full model for interaction included an empirical second-order term where the effect is modified by an interaction in the presence of both drugs.

$$\frac{d\mathbf{X}}{dt}=k_{\mathbf{syn}}\cdot\mathbf{X}\cdot\left(1-\frac{\mathbf{X}}{\mathbf{X}_{\max}}\right)-k_{\mathbf{nat}}\cdot(1+\mathbf{S}_{\max\ \ \mathbf{ATO}}\cdot C_{\mathbf{ATO}}+S_{\max\ \ \mathbf{DMAG}}\cdot C_{\mathbf{DMAG}}+\gamma\cdot C_{\mathbf{ATO}}\cdot C_{\mathbf{DMAG}})\cdot\mathbf{X};$$
$$X(0)=500,000\quad\mathbf{cells}$$
$$\frac{d\mathbf{N}_D}{dt}=k_{\mathbf{nat}}\cdot(1+\mathbf{S}_{\max\ \ \mathbf{ATO}}\cdot C_{\mathbf{ATO}}+S_{\max\ \ \mathbf{DMAG}}\cdot C_{\mathbf{DMAG}}+\gamma\cdot C_{\mathbf{ATO}}\cdot C_{\mathbf{DMAG}})\cdot\mathbf{X};\qquad N_D(0)=0\quad\mathbf{cells}\tag{7}$$

Insight into the extent of that interaction may be gained from the value of the interaction parameter, γ. If $\gamma > 0$, then there is an enhancement of effect or apparent synergy. When $\gamma < 0$, there is an apparent antagonism. When $\gamma = 0$, this is the no-interaction reference model for this interaction paradigm.

Effect was reported as percentage of viable cells. The equation is

$$\%\,\text{Viable}\quad\text{Cells}=\frac{\mathbf{X}}{\mathbf{X}+\mathbf{N}_D}\cdot 100\%\tag{8}$$

Data Analysis

Nonlinear regression fitting was performed using ADAPT II software (22). For all models, in order to resolve the pharmacological parameters (i.e. I_{max}, IC_{50}, and S_{max}) specific to each drug, single drug equations were fit to both protein expression and cell survival data for incubation with drug A alone and with drug B alone. In the case of cell-killing the base model was fit to control data with no drug to initially resolve the growth parameters of the system. These parameters were then fixed and the single drug equation was used to fit single drug data. When fitting the interaction data and employing the full interaction models, the interaction parameter is the only parameter fitted, in each model, allowing for an estimation of the potency of the interaction.

For all models, isobolograms were generated using a numerical bisection method to determine the value of drug A that produces the fifty percent effect while varying the amount of drug B in the system (23). For each concentration-effect model, isobole curves were generated for the fitted interaction and for the simulated no-interaction cases. For the no interaction isobole, the interaction term was set to its no-interaction value of one or zero.

Results

Single-Drug Effects on Protein Expression

The down-regulation of constitutive STAT3 activity by ATO, GA, 17-AAG or 17-DMAG after six hour exposure in HEL cells is shown in Figures 1 and 2. In all cases it appears that complete inhibition of PSTAT3 activity is possible at sufficiently high concentrations. Sigmoidal Emax model fittings [equation (3), ψ is fixed to 1.0] well characterized the data and the fitted parameters are listed in table 1. These plots and fittings suggest GA, with the lowest IC_{50} value of 46.8 nM, is the most potent inhibitor while ATO exhibited the least potency with an IC_{50} of 1334 nM.

Figures 1 and 3 show the up-regulation of HSP70 by ATO and the three HSP90 inhibitors. In only the case of 17-DMAG were concentrations high enough to observe a maximal effect. There appeared to be no observable differences in the tendency towards maximum stimulation of HSP70 for these drugs. HSP70 data were fit with the stimulatory model [equation (4), ψ is

fixed to 1.0 for the single drug case]. Parameters for each model fitting are reported in Table 2. Similar to PSTAT3 regulation, 17-AAG had the highest SC_{50} while GA had the lowest value. We have limited GA concentrations because it is dissolved in dimethyl sulfoxide, a solvent with known toxicity. These single-drug pharmacological effect parameters for effects on PSTAT3 and HSP70 were used in all subsequent drug-drug interaction models.

Drug-Drug Interactions on Protein Expression

The inhibitory effects of ATO in combination with the three HSP90 inhibitors on PSTAT3 expression and the surfaces representing model fittings are depicted in Figure 4. Single drug data may be observed in both the x-z and y-z planes, while points representing combinations of drugs appear in the middle of each surface. It is clear from the single drug data that complete inhibition is possible and was assumed to be the case in the model (i.e. I_{max}=1 for each drug). Both single drug and combination data were fit to equation 1 for determination of ψ, the interaction parameter. For all combinations of ATO with either GA, 17-AAG, or 17-DMAG, the fitted parameter values indicate a mechanism-based synergy as the value of ψ is less than 1.0, mutually reducing the apparent IC_{50} values of each compound for the given combination.

The stimulatory effects of ATO in combination with GA, 17-AAG, or 17-DMAG on HSP70 up-regulation and the surfaces representing model fittings are shown in Figure 5. Again, single drug data may be found in either the x-z, or y-z planes while the available data for combinations of ATO with HSP90 inhibitors tend to be clustered in the middle of the surfaces. Both single and combination data were fit to the stimulatory equation (2). The value of ψ =1.14 for GA with ATO indicates mechanism-based antagonism on HSP70 up regulation, as in combination ψ mutually increases the SC_{50} of each compound. In contrast, interactions for ATO with either 17-AAG or 17-DMAG on HSP70 expression were apparently synergistic (ψ = 0.785 and 0.654, respectively).

Isobolograms were constructed for each combination of drugs for their effects on PSTAT3 and HSP70 (Figure 6). Each line represents all possible combinations of both drugs that result in 50% of the maximal effect. The dashed lines represent the no-interaction model, or mechanism-based additivity and the solid lines represent the model fitted to the data. Interactions may be readily seen by comparing these two lines. Isobolograms for ATO in combination with the HSP90 inhibitors for their effects on both PSTAT3 and HSP70 were generated by fixing the left side of each combination model to one-half the maximal effect and solving for concentrations of the second agent as a function of the first. It is clear that the interaction line for GA and ATO on HSP70 lies outside of the no-interaction line (ψ = 1.14), meaning that more drug is required to achieve the same effect. On the other hand, for all other combinations, the interaction lines are beneath the no-interaction lines, i.e., less total drug is required to achieve the same effect.

Additionally, isobolograms allow one to discern that for different ratios of ATO and HSP90 inhibitor, the total amount of drug to achieve the same effect may vary. This is more evident for the effect on HSP70 than on PSTAT3 since these drug-drug effect-isoboles have more curvature to them. Straight isoboles indicate apparent Loewe additivity; each ratio of drug combination has the same relative total concentrations of the drugs in combination. The more the curve deviates from a straight line, the total concentration necessary to achieve the 50% effect varies for different combinations. By comparing the curvature of the different isoboles one may better understand how the interaction changes depending on the ratio of ATO to HSP90 inhibitor.

Drug-Drug Effects on Cell Survival

Cell survival at 24 and 48 hours and model fittings are shown in Figures 7A and 7B. The same concentrations were used for each incubation time. With increasing concentration it is obvious that cell survival is diminished. However, the concentrations required to observe changes in cell death are 100-1000 fold higher than those altering PSTAT3 and HSP70 protein expression. Additionally, the length of incubation time necessary to observe an effect at these higher concentrations is 4-8 times longer than that necessary for changes in protein expression. By comparing the slopes of the data on the ATO-Effect plane with the slopes of the data lying in the 17-DMAG-Effect plane, ATO appears to have a greater effect on cell death (~90-95% reduction at 48 hours) than 17-DMAG (~30% reduction at 48 hours). It is also clear that fewer cells survive during a longer incubation period for both effect curves and for the combination of ATO and 17-DMAG as well.

Data derived from 24 and 48 hours were fitted simultaneously to equation (8) incorporating in equation 7 for time-dependent drug effect. Three dimensional concentration effect surfaces were generated for each incubation time and are depicted by the mesh surfaces. Parameters for the fitting are reported in Table 3. The interaction parameter had a value of 0.0443 indicating apparent synergy. In panel 6B the synergy may actually be more pronounced than suggested by the model fitting as most of the data points lay below the surface in the center of the plot.

Isobolograms were generated to compare the concentrations required at 6, 24, and 48 hours to see the same cell-killing response (Figure 7C). Even though no cell killing was detected for the six-hour incubation, the time-dependent nature of our model allowed us to predict the concentrations necessary and the interaction at six hours (Figure 7C, black lines). The 24-hour isoboles are depicted in blue and the 48-hour isoboles are depicted in red. The dashed lines represent the no-interaction model and the solid lines represent the model fitting to the data. When comparing the dashed to the solid lines, it is clear that there is a pronounced mechanism-based synergy. Additionally, as the time of incubation increases, less amount of both drugs is required to achieve the same effect.

Isobolograms were also produced to compare joint effects of ATO and 17-DMAG on cell survival with their effects on protein expression (Figure 7D). Isobolograms permit a visual comparison of the concentrations necessary to produce the half-maximal effect, independent of the magnitude of the interaction parameters in each model. For cell killing, it is apparent from model fittings that more 17-DMAG (IC_{50} = 500 nM) is needed to kill half the cells than to down-regulate 50% of PSTAT3 (IC_{50} = 395 nM). Strikingly, for ATO, significantly more drug is needed to achieve the same cell killing effect ($IC_{50,\ 6\ hours}$ = 80,000 nM) than to down-regulate PSTAT3 (IC_{50} = 1334 nM).

Discussion

In the present study we have developed and applied pharmacodynamic models to study the hypothesis that HSP90 inhibitors will potentiate the effect(s) of ATO on constitutive STAT3 activity and cell survival in an AML cell line that constitutively expresses PSTAT3 (approximately 50% of AML cases). These models not only indicated the presence of a synergy in inhibiting PSTAT3 expression, but that this synergy occurs despite a concurrent synergy in the up-regulation of HSP70. These findings are of special significance because others have shown that up-regulation of HSP70 in an AML cell line model inhibited cytarabine and etoposide-induced apoptosis (24).

The interactions between ATO and HSP90 inhibitors have been previously studied using the Chou and Talaly method (13). However, several features of this popular approach necessitate an alternative method for assessing our drug-drug interactions. Their published equation for

the mutually exclusive case is not derived rigorously and does not adequately address the mutually non-exclusive case (17). Additionally, Chou and Talalay did not indicate how to statistically distinguish between the mutually exclusive and non-exclusive cases, through differences in effect-slope values (17). This method also uses log-linearization to simplify the analysis of the data. With the current software available, entire mechanistic equations (not requiring linearization) may be fitted by nonlinear regression, permitting statistical assessment of any interaction. Our approach is semi-mechanistic, does not require the distinction between mutually exclusive and non-exclusive interactions, and provides one statistical value indicating an overall intensity of the interaction. This semi-mechanistic pharmacodynamic model, a modified form of the Ariens non-competitive functional interaction, was used to characterize concentration-effect relationships of ATO and HSP90 inhibitors effects on PSTAT3 and HSP70 protein levels.

Mechanistic models are often applied but may be incapable of characterizing intense apparent synergy or antagonism. While mechanistically relevant; alone, this model could not predict the degree of synergy observed without the addition on a parameter to account for the interaction (ψ). The model was modified to include ψ as a mutual factor of on the EC_{50} values of both drugs. When this value was less than one, its influence on both EC_{50}s indicated that less total drug for each agent was required to achieve the same effect, an apparent mechanism-based synergy. When the value was more than one, more drug would be required indicating an apparent mechanism-based antagonism. While often empirical, the interaction parameters are useful not only for their ability to help the model capture the interaction better, but more importantly they permit a statistical measure of the interaction intensity.

The interaction parameters here were used to compare the degree of synergy between ATO and the different HSP90 inhibitors for each type of effect. For effects on PSTAT3 inhibition, the combination of ATO and GA had the lowest value of ψ (0.662) indicating in the model that it took much less drug to achieve the same effect when compared to the other combinations. It is of interest that the most synergistic interaction affecting PSTAT3 (GA and ATO) had antagonistic effect on HSP70 (ψ=1.14). This is the first comparison of the three HSP90 inhibitors with ATO; we do not have an explanation for this finding as we expected that inhibiting PSTAT3 will result in concomitant up-regulation of HSP70, as was seen with the other HSP90 inhibitors. Smith and colleagues (25) showed that *in vitro* comparison of 17-AAG and 17-DMAG, the two inhibitors that are being tested in clinical trials, resulted in more pronounced effect for 17-DMAG. Our results concur with these findings; the ψ value for both inhibiting PSTAT3 and stimulating HSP70 were lower for 17-DMAG, indicating that much less drug was needed to achieve the same effect when compared to the other combination.

The analysis of the effects of these drugs on cell survival was limited to the combination of ATO and 17-DMAG due to better solubility of 17-DMAG in aqueous solutions and hence potential use in clinical trials. Cell survival studies with ATO and 17-DMAG were done to determine whether the synergy observed on PSTAT3 regulation was indeed a direct interaction on PSTAT3 regulation and not a synergy resulting from cell death. Interestingly, cell survival studies showed no significant drug effect after six-hour incubation. Therefore, incubations were extended for 24 and 48 hours. The resulting data is time-dependent, adding a fourth dimension. A mechanistic model for cell-killing with an interaction term, similar to the modified functional interaction used previously, was developed to explain differences in a time-dependent manner. The model structures between cell survival and protein level differed significantly and any comparison of the interaction terms would certainly not yield the same degree of interaction. Therefore, isobolograms were used to compare the interaction between protein regulation at six hours and the mechanistic time-dependent model prediction of cell killing at six hours.

Isobolograms are useful since they allow a comparison of interactions between different types of effects. The lines in these plots represent all the combinations required to achieve a particular effect level (i.e. 50% of the maximal effect). Interactions for two different effects (with different scales or effect units) may be compared at one level (e.g. 50% maximal) by identifying the amount of each drug, for a given combination, required to elicit that response level. We used the isobolograms to compare the interactions between ATO and 17-DMAG on cell survival and PSTAT3 protein level following six-hour incubation. Our results demonstrate that at six hours, the amount of drugs required to down-regulate PSTAT3 is significantly lower than the amount needed to cause cell death. These results suggest that combinations of these agents will need to be administered over prolonged periods of time to achieve cell death. Alternatively, these agents can be administered over a short period of time to down-regulate constitutive STAT3 activity and thus potentiate the effect of other drugs used to treat AML.

The IC_{50} values in our models were within the physiologic ranges [ATO (26,27), 17-AAG (28) and 17-DMAG (29,30)]. However, the drug effect was measured and modeled not only for the physiologically relevant concentrations but also beyond. Even then, some of the graphs do not display a maximum effect in the observed data. We caution regarding the utility of these models beyond the presented range of concentrations, as the maximal effect often influences the determination of other parameters such as EC_{50}.

In summary, Parmar and colleagues (31) have shown that ATO alone, though effective *in vitro* in inducing apoptosis of AML cells, is not sufficiently effective *in vivo* in inducing remission in AML patients. Therefore, combination trials are needed. It is of interest that HSP90 inhibition sensitized AML cells to cytarabine *in vitro* (32). Finally, the combination of ATO with the HSP90 inhibitor, 17-AAG, has shown some promise *in vitro* (13) but the pharmacodynamic modeling was not appropriate to address the mechanistic questions that the combination of these two type of drugs present. Of interest is the fact that both approaches, the one studying the interaction as a mutually exclusive case (13) and the one taking the mechanistic approach (current), reached the same conclusion. This supports further testing of combinations of ATO and 17-AAG or preferably 17-DMAG in pre-clinical AML *in vivo* models.

Acknowledgments

Supported partially by grants from the National Cancer Institute Grants CA16056 and CA99238, NIH Grant GM57980 and by The Heidi Leukemia Research Fund (Buffalo, NY).

REFERENCES

1. Benekli M, Xia Z, Donohue KA, Ford LA, Pixley LA, Baer MR, Baumann H, Wetzler M. Constitutive activity of signal transducer and activator of transcription 3 protein in acute myeloid leukemia blasts is associated with short disease-free survival. Blood 2002;99:252–257. [PubMed: 11756179]
2. Wetzler M, Brady MT, Tracy E, Li ZR, Donohue KA, O'Loughli KL, Cheng Y, Mortazavi A, McDonald AA, Kunapuli P, Wallace PK, Baer MR, Cowell JK, Baumann H. Arsenic trioxide affects signal transducer and activator of transcription proteins through alteration of protein tyrosine kinase phosphorylation. Clin Cancer Res. 2006
3. Whitesell L, Lindquist SL. HSP90 and the chaperoning of cancer. Nat Rev Cancer 2005;5:761–772. [PubMed: 16175177]
4. Takayama S, Reed JC, Homma S. Heat-shock proteins as regulators of apoptosis. Oncogene 2003;22:9041–9047. [PubMed: 14663482]
5. Beere HM. "The stress of dying": the role of heat shock proteins in the regulation of apoptosis. J Cell Sci 2004;117:2641–2651. [PubMed: 15169835]

6. Yu D, Wang ZH, Cheng SB, Li HK, Chan HB, Chew EC. The effect of arsenic trioxide on the expression of Hsc and HNF4 in nuclear matrix proteins in HepG2 cells. Anticancer Res 2001;21:2553–2559. [PubMed: 11724321]
7. Tchounwou PB, Yedjou CG, Dorsey WC. Arsenic trioxide-induced transcriptional activation of stress genes and expression of related proteins in human liver carcinoma cells (HepG2). Cell Mol Biol (Noisy-le-grand) 2003;49:1071–1079. [PubMed: 14682389]
8. Saulle E, Riccioni R, Pelosi E, Stafness M, Mariani G, De Tuglie G, Peschle C, Testa U. In vitro dual effect of arsenic trioxide on hemopoiesis: Inhibition of erythropoiesis and stimulation of megakaryocytic maturation. Blood Cells Mol Dis 2006;36:59–76. [PubMed: 16360329]
9. Shen HY, He JC, Wang Y, Huang QY, Chen JF. Geldanamycin induces heat shock protein 70 and protects against MPTP-induced dopaminergic neurotoxicity in mice. J Biol Chem 2005;280:39962–39969. [PubMed: 16210323]
10. Guo F, Rocha K, Bali P, Pranpat M, Fiskus W, Boyapalle S, Kumaraswamy S, Balasis M, Greedy B, Armitage ES, Lawrence N, Bhalla K. Abrogation of heat shock protein 70 induction as a strategy to increase antileukemia activity of heat shock protein 90 inhibitor 17-allylamino-demethoxy geldanamycin. Cancer Res 2005;65:10536–10544. [PubMed: 16288046]
11. Loewe S, Muischnek H. Über kombinationswirkungen. I. Mitteilung: hilsfmittel der fragestelllung. Arch Exp Path Pharmakol 1926;114:313–326.
12. Bliss CI. The toxicity of poisons applied jointly. Ann Appl Biol 1939;26:585–615.
13. Pelicano H, Carew JS, McQueen TJ, Andreeff M, Plunkett W, Keating MJ, Huang P. Targeting Hsp90 by 17-AAG in leukemia cells: mechanisms for synergistic and antagonistic drug combinations with arsenic trioxide and Ara-C. Leukemia 2006;20:610–619. [PubMed: 16482209]
14. Chou TC, Talalay P. Quantitative analysis of dose-effect relationships: the combined effects of multiple drugs or enzyme inhibitors. Adv Enzyme Regul 1984;22:27–55. [PubMed: 6382953]
15. Ariens EJ, Simonis AM. A molecular basis for drug action. J Pharm Pharmacol 1964;16:137–157. [PubMed: 14163978]
16. Ariens EJ, Van Rossum JM, Simonis AM. Affinity, intrinsic activity and drug interactions. Pharmacol Rev 1957;9:218–236. [PubMed: 13465302]
17. Greco WR, Bravo G, Parsons JC. The search for synergy: a critical review from a response surface perspective. Pharmacol Rev 1995;47:331–385. [PubMed: 7568331]
18. Chakraborty A, Jusko W,J. Pharmacodynamic interaction of recombinant human interleukin-10 and prednisolone using in vitro whole blood lymphocyte proliferation. J Pharm Sci 2002;91:1334–1342. [PubMed: 11977109]
19. Chow FS, Jusko WJ. Immunosuppressive interactions among calcium channel antagonists and selected corticosteroids and macrolides using human whole blood lymphocytes. Drug Metab Pharmacokinet 2004;19:413–421. [PubMed: 15681895]
20. Xia Z, Baer MR, Block AW, Baumann H, Wetzler M. Expression of signal transducers and activators of transcription proteins in acute myeloid leukemia blasts. Cancer Res 1998;58:3173–3180. [PubMed: 9679986]
21. Xia Z, Salzler RR, Kunz DP, Baer MR, Kazim L, Baumann H, Wetzler M. A novel serine-dependent proteolytic activity is responsible for truncated signal transducer and activator of transcription proteins in acute myeloid leukemia blasts. Cancer Res 2001;61:1747–1753. [PubMed: 11245492]
22. D'Argenio, DZ.; Schumitzky, A. ADAPT II Users guide: Pharmacokinetc/pharmacodynamic systems analysis software. Biomedical Simulations Resource; Los Angeles: 1997.
23. Press, WH.; Teukolsky, WT.; Velterling, WT.; Flannery, BP. Numerical Recipes in Fortran 77. Vol. Second Edition. Cambridge University Press; New York, NY: 1992. p. 343-346.
24. Guo F, Sigua C, Bali P, George P, Fiskus W, Scuto A, Annavarapu S, Mouttaki A, Sondarva G, Wei S, Wu J, Djeu J, Bhalla K. Mechanistic role of heat shock protein 70 in Bcr-Abl-mediated resistance to apoptosis in human acute leukemia cells. Blood 2005;105:1246–1255. [PubMed: 15388581]
25. Smith V, Sausville EA, Camalier RF, Fiebig HH, Burger AM. Comparison of 17-dimethylaminoethylamino-17-demethoxy-geldanamycin (17DMAG) and 17-allylamino-17-demethoxygeldanamycin (17AAG) in vitro: effects on Hsp90 and client proteins in melanoma models. Cancer Chemother Pharmacol 2005;56:126–137. [PubMed: 15841378]

26. Shen ZX, Chen GQ, Ni JH, Li XS, Xiong SM, Qiu QY, Zhu J, Tang W, Sun GL, Yang KQ, Chen Y, Zhou L, Fang ZW, Wang YT, Ma J, Zhang P, Zhang TD, Chen SJ, Chen Z, Wang ZY. Use of arsenic trioxide (As2O3) in the treatment of acute promyelocytic leukemia (APL): II. Clinical efficacy and pharmacokinetics in relapsed patients. Blood 1997;89:3354–3360. [PubMed: 9129042]

27. Shen Y, Shen ZX, Yan H, Chen J, Zeng XY, Li JM, Li XS, Wu W, Xiong SM, Zhao WL, Tang W, Wu F, Liu YF, Niu C, Wang ZY, Chen SJ, Chen Z. Studies on the clinical efficacy and pharmacokinetics of low-dose arsenic trioxide in the treatment of relapsed acute promyelocytic leukemia: a comparison with conventional dosage. Leukemia 2001;15:735–741. [PubMed: 11368433]

28. Egorin MJ, Zuhowski EG, Rosen DM, Sentz DL, Covey JM, Eiseman JL. Plasma pharmacokinetics and tissue distribution of 17-(allylamino)-17-demethoxygeldanamycin (NSC 330507) in CD2F1 mice1. Cancer Chemother Pharmacol 2001;47:291–302. [PubMed: 11345645]

29. Egorin MJ, Lagattuta TF, Hamburger DR, Covey JM, White KD, Musser SM, Eiseman JL. Pharmacokinetics, tissue distribution, and metabolism of 17-(dimethylaminoethylamino)-17-demethoxygeldanamycin (NSC 707545) in CD2F1 mice and Fischer 344 rats. Cancer Chemother Pharmacol 2002;49:7–19. [PubMed: 11855755]

30. Glaze ER, Lambert AL, Smith AC, Page JG, Johnson WD, McCormick DL, Brown AP, Levine BS, Covey JM, Egorin MJ, Eiseman JL, Holleran JL, Sausville EA, Tomaszewski JE. Preclinical toxicity of a geldanamycin analog, 17-(dimethylaminoethylamino)-17-demethoxygeldanamycin (17-DMAG), in rats and dogs: potential clinical relevance. Cancer Chemother Pharmacol 2005;56:637–647. [PubMed: 15986212]

31. Parmar S, Rundhaugen LM, Boehlke L, Riley M, Nabhan C, Raji A, Frater JL, Tallman MS. Phase II trial of arsenic trioxide in relapsed and refractory acute myeloid leukemia, secondary leukemia and/or newly diagnosed patients at least 65 years old. Leuk Res 2004;28:909–919. [PubMed: 15234567]

32. Mesa RA, Loegering D, Powell HL, Flatten K, Arlander SJ, Dai NT, Heldebrant MP, Vroman BT, Smith BD, Karp JE, Eyck CJ, Erlichman C, Kaufmann SH, Karnitz LM. Heat shock protein 90 inhibition sensitizes acute myelogenous leukemia cells to cytarabine. Blood 2005;106:318–327. [PubMed: 15784732]

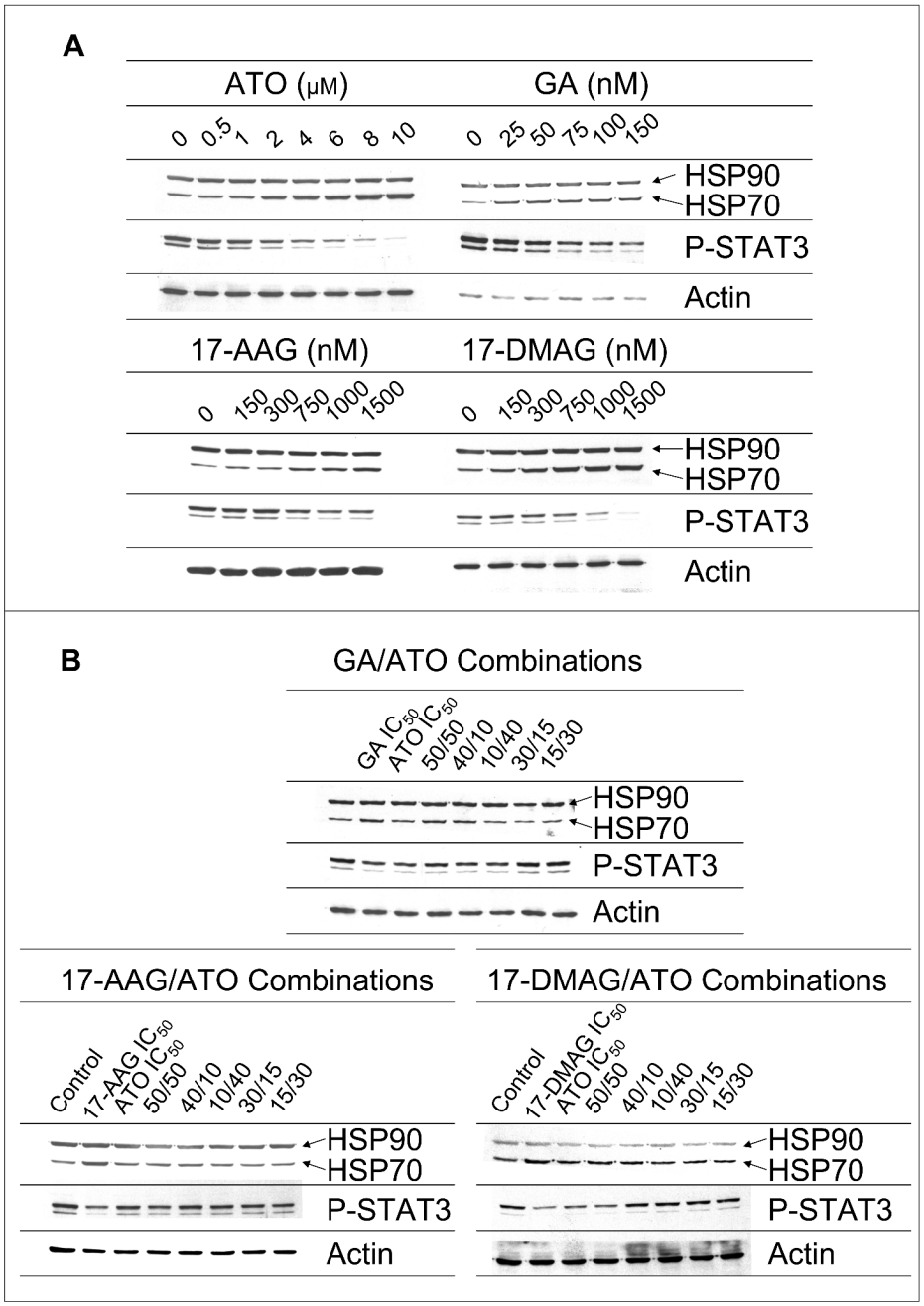

Figure 1.
The dose-dependent effect of ATO and the HSP90 inhibitors, GA, 17-AAG and 17-DMAG, alone (A) and in combination (B), on HSP70, HSP90 and constitutive STAT3 protein activity.

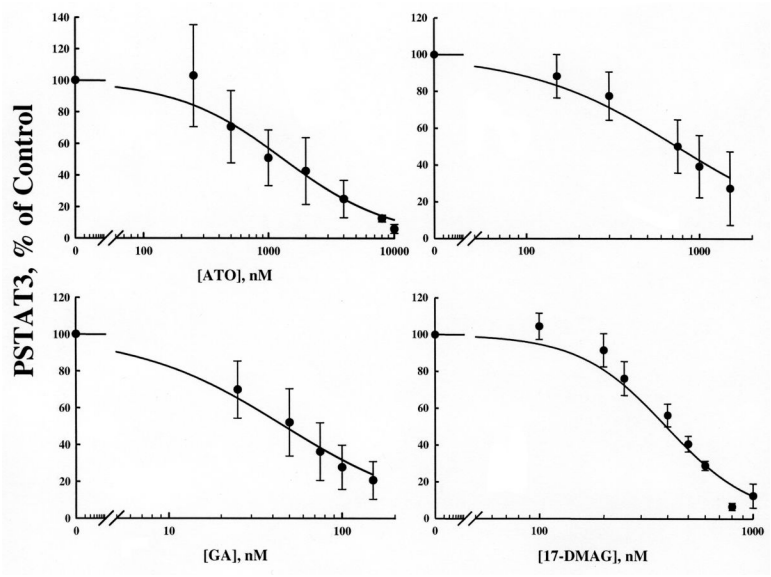

Figure 2.

Single drug response curves for the effects of ATO in combination with HSP90 inhibitors GA, 17-AAG, and 17-DMAG on the down-regulation of PSTAT3 expression. Solid lines represent model prediction (Eq. 3). Closed circles are observed mean data ± standard deviation (SD).

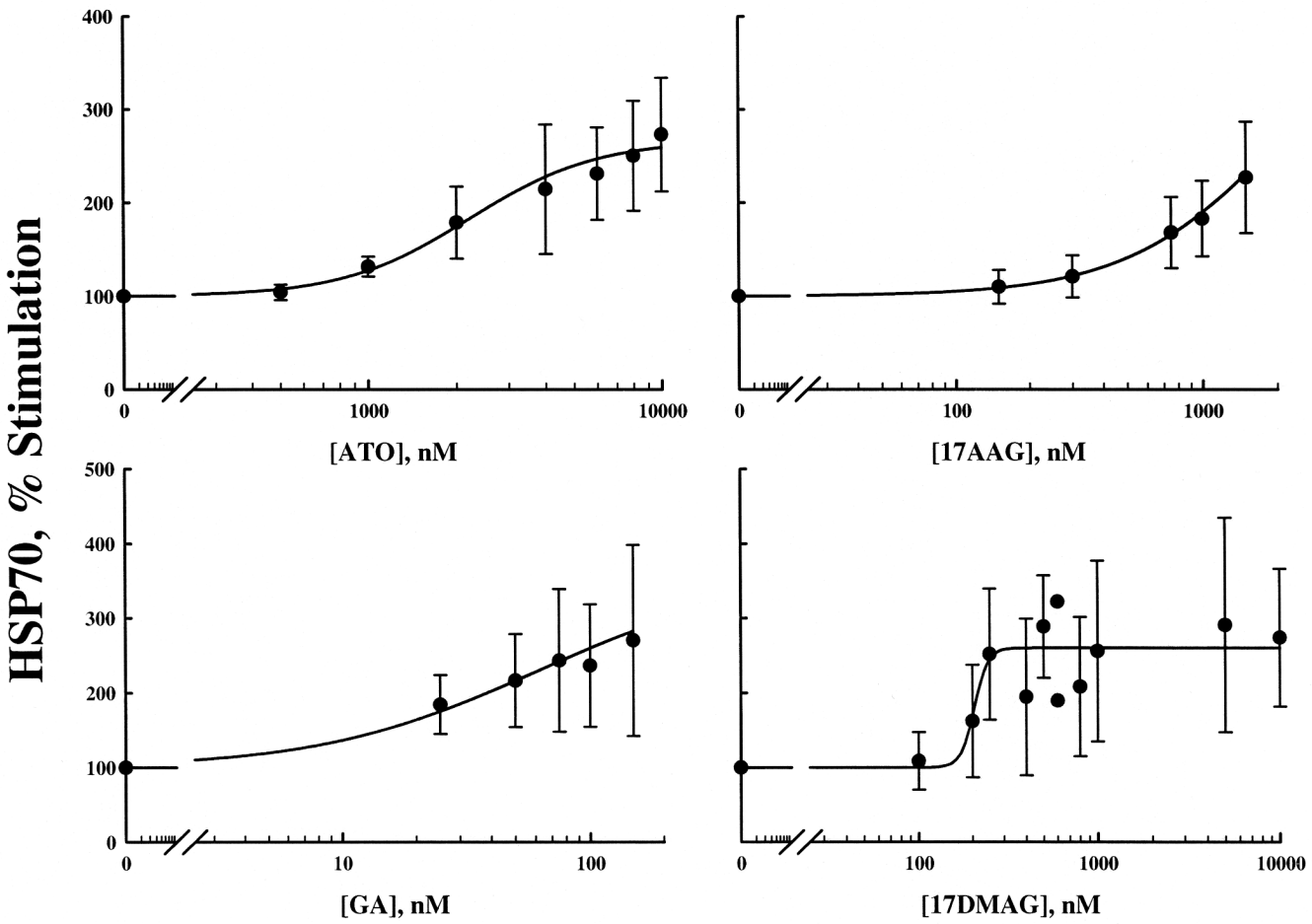

Figure 3.
Single drug response curves for the effects of ATO in combination with HSP90 inhibitors GA, 17-AAG, and 17-DMAG on the up-regulation of HSP70 expression (Eq. 4). Closed circles are observed mean data ± SD.

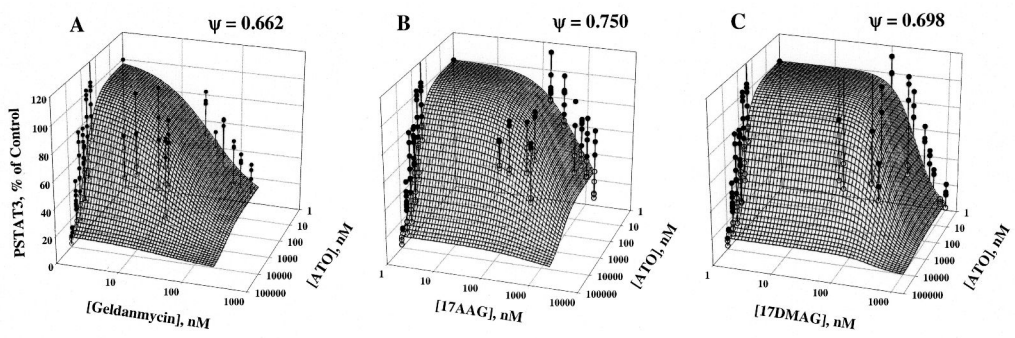

Figure 4.

Three-Dimensional plots of drug effect on PSTAT3 expression for ATO and GA, 17-AAG, or 17-DMAG in combination. Mesh surfaces are the theoretical model predictions based on the parameters fitted to the experimental data (Eq. 1). Solid circles represent observed points above the surface and open circles represent observed data below the predicted surface. Vertical lines indicate distance to surface and position.

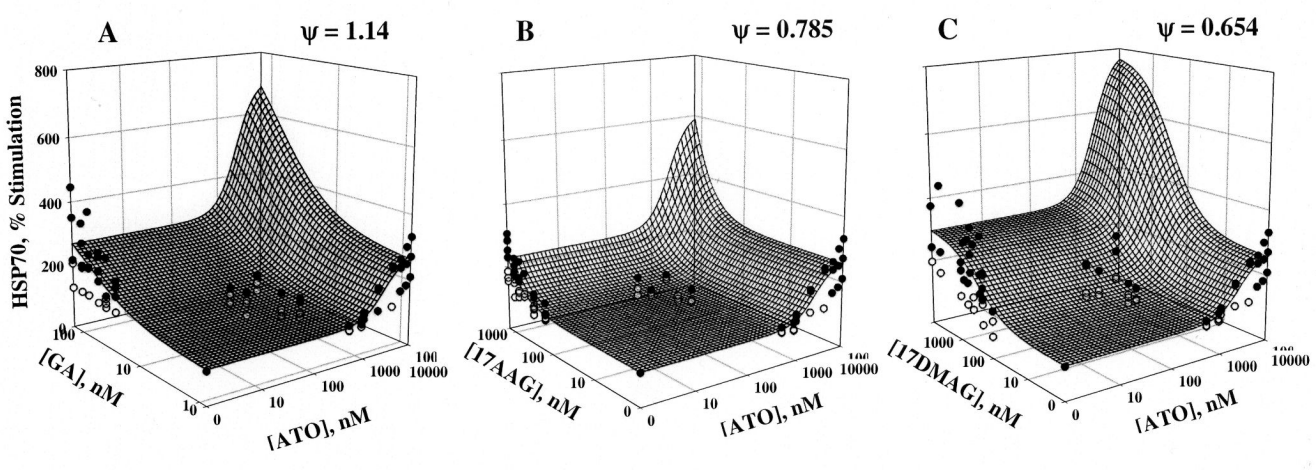

Figure 5.

Three-Dimensional plots of drug effect on HSP70 expression for ATO and GA, 17-AAG, or 17-DMAG in combination. Mesh surfaces are the theoretical model predictions based on the parameters fitted to the experimental data (Eq. 2). Solid circles represent observed points above the surface and open circles represent observed data below the predicted surface.

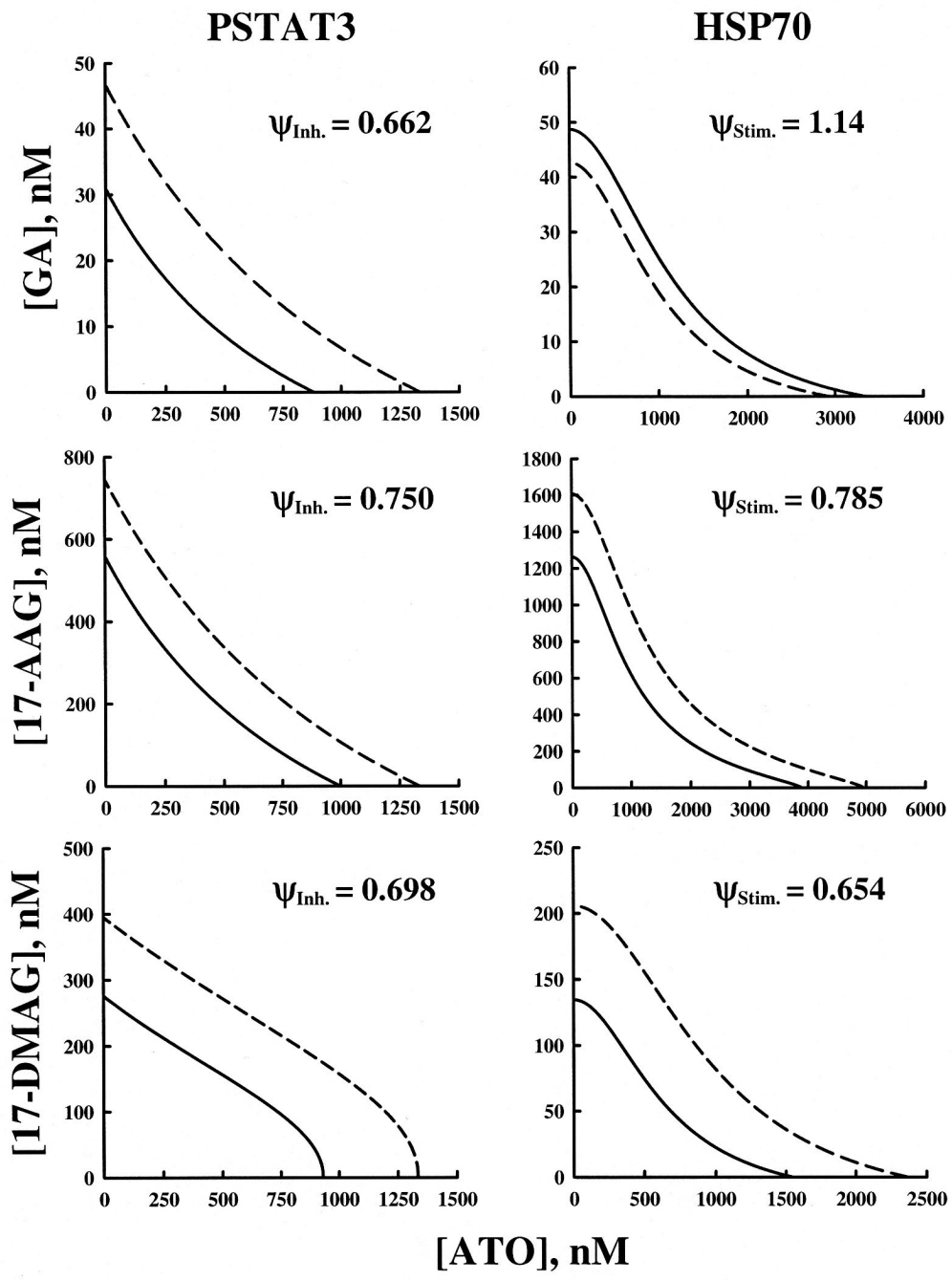

Figure 6.

Isobologram for the effects of ATO and HSP inhibitors GA, 17-AAG, and 17-DMAG in combination on inhibition of PSTAT3 expression (left panel), and stimulation of HSP70 expression (right panel). Solid lines represent the predicted interaction curve where the value of interaction parameter is fitted (Eq. 7,8). The dashed line represents mechanism-based additivity expected if no interaction were to exist ($\psi = 1$). Final estimates of the interaction parameter (ψ) values are presented for both inhibitory and stimulatory effects.

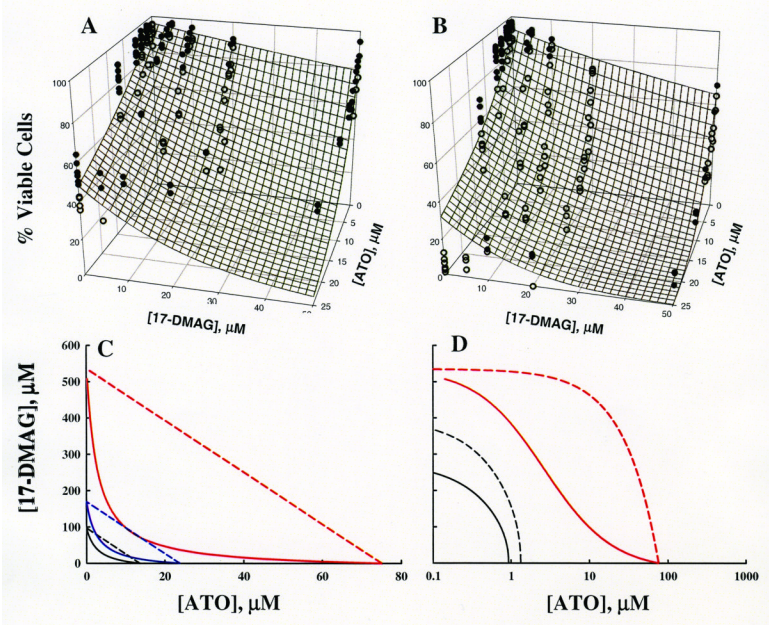

Figure 7.

Model fitting of cell survival data. The mesh surface is the model prediction at 24 hours (A) and 48 hours (B). Solid circles are data points above the surface. Open circles represent data points below the surface. (C) Isobolograms for 50% cell survival at 6, 12, and 48 hours. Solid lines display isobole curves for the predicted cell killing interaction model. Dashed lines represent the additive isobole when the interaction parameter is set to its no-interaction value, zero. Model predictions are shown for 50% cell survival with 6 hour (red lines), 24 hour (blue lines), and 48 hour (black lines) incubations. (D) Six hour isobolograms for 50% cell survival (red) compared to those for 50% PSTAT3 down-regulation (black). Dashed lines indicate the no-interaction curve. Solid lines are model fittings [Eq. 1 (black lines) and Eq. 7, 8 (red lines)]. The x-axis is log scale for visualizing all curves.

Table 1

Parameter estimates for single-drug effects on P-STAT3 down-regulation.

Drug	IC_{50} (nM)	CV%	Hill Coefficient	CV%
ATO	1334	9.917	N/A	N/A
GA	46.81	12.08	N/A	N/A
17-AAG	744.8	10.21	N/A	N/A
17-DMAG	395	7.221	2.115	10.47

Table 2

Parameter estimates for single-drug effects on HSP70 up-regulation.

Drug	S_{max}	CV%	SC_{50} (nM)	CV%	Hill Coefficient	CV%
ATO	1.67	15.2	2220	27.3	2.03	33.5
GA	2.56	32.7	60.2	71.5	N/A	N/A
17-AAG	3.55	152	2220	185	1.36	40.1
17-DMAG	2.03	17.9	266	51.7	N/A	N/A

Table 3

Parameter estimates for single and combined drug effects of ATO and 17-DMAG on cell-survival.

Parameter	Parameter Description	Estimate	CV%
$S_{max,ATO}$	Cell-Killing Rate Constant For ATO	0.845	7.8
$S_{max,17\text{-}DMAG}$	Cell-Killing Rate Constant For 17-DMAG	0.118	15
k_{syn}	Natural Cell Synthesis Rate Constant	0.0671	N/A
X_{max}	Maximal Number of Cells	1530	N/A
k_{nat}	Rate of Natural Cell-Death	0.00202	N/A
γ	Interaction Parameter	0.0443	18.3